G53168R

Greenlandic debris in Iceland likely tied to Bond 1 ice-rafting in the Dark Ages

Christopher J. Spencer[1]*, Thomas M. Gernon[2], Ross N. Mitchell[3,4]

[1] Department of Geological Sciences and Geological Engineering, Queen's University, Kingston, Ontario, Canada

[2] School of Ocean & Earth Science, University of Southampton, Southampton, UK

[3] State Key Laboratory of Lithospheric and Environmental Coevolution, Institute of Geology and Geophysics, Chinese Academy of Sciences, Beijing 100029, China

[4] College of Earth and Planetary Science, University of Chinese Academy of Sciences, Beijing 100049, China

*Email: c.spencer@queensu.ca

ABSTRACT

We report the discovery of exotic igneous, metamorphic, and sedimentary cobbles in raised beach deposits near Breiðavík, northern Iceland. These deposits consist of alternating cobble-, sand-, and silt-dominated facies. A nearby package of sands and silts, dated to the Late Antique Little Ice Age (LALIA; ca. 536–660 CE), provides age constraints for the raised terraces. While the upper terraces are composed exclusively of local basaltic material, the lowermost terraces (~2 m above high tide) contain a mix of basaltic and non-basaltic cobbles, including quartzofeldspathic gneiss, granitoid, rhyolite, sandstone, and serpentinite. U–Pb geochronology of zircon reveals dominant age modes of ca. 2800, 1150, 500, and 240 Ma with Lu–Hf isotopic compositions suggesting derivation from Greenland's North Atlantic Craton and Caledonian fold belt.

The colder conditions of the LALIA, coupled with increased iceberg calving from the Greenland Ice Sheet, would have led to enhanced ice-rafted debris (IRD) transport to disparate areas south and east of Greenland. The East Greenland and East Iceland currents transported this IRD from Greenland, with deposition occurring along the Icelandic coast as the icebergs melted. This IRD was likely transported across the North Atlantic during Bond Event 1. This process, along with those during other transient cooling events, may explain the age discrepancies between local bedrock and detrital zircons in the Arctic.

INTRODUCTION

During the Last Glacial Maximum (LGM), ca. 26,000–19,000 years ago, ice sheets extended across much of the Northern Hemisphere, dramatically reshaping the landscape by locally carving bedrocks and depositing glacial regolith. These ice sheets were highly dynamic, advancing and retreating in response to climatic shifts, and transporting large volumes of glacial debris into the marine environment (Batchelor et al., 2019). Following the LGM, shorter-term climate oscillations, such as the Bond events, involved continued fluctuations in the Northern Hemisphere's climate over the past 11,500 years (Bond et al., 1993, 2001). These recurring cold phases, likely linked to changes in ocean circulation and solar activity, intensified glaciation and influenced ice-rafted debris (IRD) transport. For instance, Bond Event 1, which coincides with the Late Antique Little Ice Age (LALIA; 536–660 CE after Büntgen et al., 2016), saw a renewed expansion of the Greenland Ice Sheet (Büntgen et al., 2016; Kjær et al., 2022). These episodes of climate-driven glaciation and deglaciation highlight the persistent influence of millennial-scale climate shifts on glacial systems and their role in shaping

the landscapes and sedimentary records of the North Atlantic region (Büntgen et al., 2016).

IRD refers to sedimentary material transported by icebergs or sea ice that is released into marine or coastal environments when the ice melts. IRD is a key proxy for understanding past glacial activity and ocean circulation, as its range of materials often reflects the diverse geology of source regions. Icebergs calved from glaciers can carry debris as varied as local sediments, large boulders, and exotic rock fragments sourced from the heart of continental interiors (Gilbert, 1990). As icebergs drift with ocean currents, they can transport these materials hundreds to thousands of kilometers before melting and depositing their debris load. IRD is commonly found in ocean sediments throughout the Northern Hemisphere, particularly in the North Atlantic region, where icebergs predominately originate from the Greenland Ice Sheet and other Arctic glaciers. Previous studies of IRD in North Atlantic drill cores have revealed a remarkable geological diversity (Eldrett et al., 2007; White et al., 2016; Darby et al., 2017), much of which is traceable to Greenland’s geological provinces. These studies have shown how IRD provides snapshots of glacial dynamics, with debris originating from distinct geologic formations across Greenland and other northern landmasses, such as Svalbard and Scandinavia. Through compositional analyses of IRD, it is possible to pinpoint provenances and reconstruct past iceberg trajectories, ocean current patterns, and the timing of glacial advances and retreats (White et al., 2016).

What makes IRD particularly significant is its ability to transport exotic materials far from their points of origin, often to locations where the local bedrock contrasts starkly with the incoming debris (Heinrich, 1988). This process not only provides insights into glacial

transport but also serves as a marker of long-distance oceanic sedimentation (Bailey et al., 2012). The presence of foreign geological material in ocean sediments often highlights the expansive reach of glacial systems and their interaction with ocean currents during glacial periods.

However, while the transport of IRD across ocean basins is well documented (Bailey et al., 2012; White et al., 2016), there is less understanding of its deposition on subaerial continental environments. This raises important questions about the processes involved when exotic material, particularly from Greenland, reaches landmasses such as Iceland—a region dominated by recent basaltic volcanism rather than ancient continental geology. Here, we present newly discovered non-basaltic material in northern Iceland in the Breiðavík region. Through zircon U–Pb geochronology and Lu–Hf isotopic analyses, we identify a range of igneous and metamorphic rock types with ages and isotopic compositions matching those of Greenlandic provinces. Fingerprinting of these exotic Greenland-derived clasts in Iceland provides insights into the nature of late Quaternary IRD at the boundary between the North Atlantic and Arctic oceans.

GEOLOGIC SETTING

Iceland, situated on the Mid-Atlantic Ridge with a supporting mantle plume, is a geologically young and dynamic island characterized by basaltic lava flows and minor evolved magmas, driven by seafloor spreading and mantle plume magmatism (Foulger et al., 2022). The Westfjords in northwest Iceland are among the island's oldest regions, primarily composed of 10–16 Ma basalt lavas, contrasting with the younger central volcanic areas. The region is highly eroded, with steep, fjord-lined coastlines that reflect glacial activity during the Pleistocene. The ice sheets that once covered the Westfjords

during the LGM contributed to the formation of these deep fjords, as glaciers carved through the landscape, leaving behind distinctive U-shaped valleys. Despite its volcanic origins, the Westfjords are notable for their lack of recent volcanic activity compared to other parts of Iceland, contributing to a more stable, though heavily glaciated, geologic environment.

The Breiðavík region, located along the northern coastline of the Westfjords, features beach deposits consisting of alternating sand and silt, and cobble layers with two distinct terraces above the high-tide line (Fig. 1A). The higher terrace is primarily composed of local basaltic material, likely sourced from nearby volcanic flows. In contrast, the lowermost terraces, closer to present-day sea levels (Fig. 1B), contain a mix of basaltic and non-basaltic rocks, with the non-basaltic material being the focus of this study. This distinct stratigraphy suggests multiple phases of deposition, likely tied to glacial retreat and the influx of offshore sediments. The origin of these terraces has been linked to stages of deglaciation and subsequent isostatic uplift, and sands and silts at a similar level (that is, approximately 4 m above mean sea level) exposed to the southwest of the Breiðavík Bay were formed ca. 1,300–1,400 years BP (Brader et al., 2017). Corresponding to ca. 600–700 AD, these dates align with Bond Event 1 and the Late Antique Little Ice Age, which likely enhanced iceberg calving and IRD transport (Savkina et al., 2018). While not definitive, this date offers a valuable age constraint that aligns with geological observations of the raised beach context and the presence of extraneous, likely ice-transported material.

Across the Denmark Strait from Iceland is East Greenland (Fig. 2), whose geology is characterized by diverse lithologies spanning Mesoarchean orthogneiss to Paleogene

flood basalts. East Greenland's geology is defined by four primary regions (from south to north): the Paleoproterozoic Ketilidian Mobile Belt (Vestergaard et al., 2024), orthogneisses of the Archean Block (Kolb et al., 2013), the Nagssugtoqidian Mobile Belt (Nutman et al., 2008), Paleogene mafic magmatism (Brooks, 2011), and the Paleozoic Caledonian Fold Belt (Rehnström, 2010). Except for the Caledonides, the geology in western Greenland broadly mirrors that of eastern Greenland (White et al., 2016). Modern iceberg sources include major calving regions such as Disko Bugt in western Greenland and the Scoresby Sound system in the east. These regions contribute substantially to the annual flux of icebergs into the North Atlantic (Rignot and Kanagaratnam, 2006). Icebergs transported by the East Greenland Current (EGC) carry IRD southward, while local sources dominate IRD deposition in marine-proximal environments (Andrews et al., 2014). This study focuses on reconstructing the provenance of IRD deposited on raised beaches near Breiðavík to discern the relative contributions of Greenlandic source terrains.

SAMPLES AND METHODS

Samples were collected from recent beach deposits near Breiðavík in northern Iceland. The deposits consist of alternating cobble- and sand-dominated facies, with an upper terrace comprised exclusively of basaltic material and a lower terrace containing a mixture of basaltic and non-basaltic cobbles. The lower terrace sits ~2 m below the isolation basin (~2 m a.s.l.) on the western side of the bay sampled by Brader et al. (2017) corresponding to the horizon dated at 1301–1407 BP. Among the cobble samples collected, those for which zircon separation was done include a sandstone, seven (meta)granitoids, and two felsic volcanics. The sandstone is medium-grained,

well-sorted, and quartz-rich. The (meta)granitoids are medium- to coarse-grained and exhibit variable degrees of deformation and metamorphism. The felsic volcanics are gray and ochre, fine-grained volcanic rocks rich in silica, typically rhyolite or dacite in composition. Other collected samples include two mafic volcanics, two fine-grained siliciclastic rocks, four quartzite/quartz-rich cobbles, and one serpentinized peridotite. Standard zircon separation and U–Pb/trace element/Hf split stream by LA-ICPMS methods were used and are detailed in the Supplementary Materials.

ZIRCON U–Pb AND Hf ISOTOPE RESULTS

U–Pb ages from zircon grains from the Breiðavík beach clasts reveal multiple distinct age populations. Zircon ages from the clasts range from 2960 Ma and 0 Ma with major age frequency peaks at 2800 Ma, 1150 Ma, 500 Ma, 240 Ma, and 0 Ma and subordinate peaks at 1600 Ma, 1380 Ma, 720 Ma, and 370 Ma (Fig. 3). Hafnium isotopes of zircon show a broad range of εHf values (Fig. 3). The Archean ages have εHf that range from 4 to -6 (-2 average), εHf of Proterozoic ages range from 6 to -8 (1.5 average), Cambrian to Devonian ages have εHf that range from 3 to -9 (-3 average), Carboniferous to Cretaceous ages have bimodal εHf with a more depleted population at 4 to 11 (8 average) and an enriched population at -3 to 1 (-1 average), two Neogene grains have an average εHf of 12, and Quaternary ages have εHf of 1 to 5 (3 average).

DISCUSSION

Comparison with Greenlandic sources

The Breiðavík clasts' zircon age and εHf populations closely resemble those reported from known Greenlandic geological terrains, except for the post-Devonian population

(Fig. 3). The Archean zircons correspond well with known ages and εHf of the North Atlantic Craton (Johnston and Kylander-Clark, 2013; Nicoli et al., 2018), while the Proterozoic ages and εHf can be linked to the Ketitlides and detritus linked to the Grenville Orogeny (Olierook et al., 2020). Cambrian–Devonian ages and εHf are most closely similar to the Caledonides (Rehnström, 2010; Brueckner et al., 2016) though the most enriched εHf values are not represented in the Breiðavík clasts. This raises the possibility of additional, more distant sources, such as Siberia or the Sverdrup basin, which host detrital zircon with similar age and Hf isotopic characteristics (Røhr et al., 2010). These regions, known for their late Paleozoic and Mesozoic magmatism, plausibly contributed material via trans-Arctic glacial or oceanic transport mechanisms, suggesting a more complex pattern of sediment provenance than previously thought.

Implications for sediment provenance and IRD transport

The age and isotopic diversity of the studied zircons offer new insights into the region's IRD history. The presence of both ancient Archean cobbles and more recent Mesozoic zircon points to a mixture of sources, likely including Greenlandic basement rocks and younger, perhaps rift-related volcanic material. This mixture of zircon ages suggests that sedimentary material was transported across the North Atlantic, most likely as IRD, and subsequently deposited along the Icelandic coast. As icebergs drifted into the waters around Iceland, they would have encountered the warmer Irminger Current, the western North Atlantic branch of the Gulf Stream Current flowing north along Iceland's western coast (Fig. 2; Perner et al., 2016). This warmer current likely accelerated melting, causing the icebergs to 'dump' debris. Clasts dropped by icebergs, whether angular or

rounded and with or without striations (Gilbert, 1990), were likely shaped to some extent by wave action before deposition.

The Hf isotopic data further support a Greenlandic provenance, showing a wide range of εHf values consistent with multiple crustal and mantle-derived sources (Fig. 3). The wide ranges in ages and isotopes likely reflects the mixing of lithologies in moraines and glacial tills, sampling different catchments, and originating from many iceberg 'dump' events offshore Iceland. Importantly, the IRD-rich terrace from Breiðavík correlates with an isolation basin corresponding to Bond Event 1 (1,301–1,407 cal. BP) (Brader et al., 2017), which is tied to the LALIA, spanning from ca. 536–660 CE (Büntgen et al., 2016). Further support for an increase in Greenlandic IRD flux during this time comes from a peak in hematite-stained quartz observed in sediment cores offshore Iceland and the IRD >2 mm in the Nansen Trough (Andrews et al., 2014). Notably, the LALIA coincides with intensified volcanic activity, including a large eruption in Iceland around 536 CE (Büntgen et al., 2022). Those volcanic eruptions and subsequent climatic cooling are believed to have triggered an expansion of the Greenland Ice Sheet (Kjær et al., 2022), likely contributing to enhanced iceberg calving.

The combined influences of the East Greenland current (EGC) and East Icelandic current (EIC), modulated by the colder climatic conditions of the LALIA, likely facilitated the southward transport of Greenlandic IRD along Iceland's coastal margins (Fig. 2; White et al., 2016). However, the deposition was probably influenced by the warmer Irminger current, which would have played a critical role in distributing and depositing IRD in these regions through interactions with the colder currents (Knudsen et al., 2004). We have now documented an even more diverse assemblage of crustal

materials, linked directly to East Greenland. While there is great potential to use zircon to evaluate the prospect of ancient continental crust beneath Iceland (Foulger et al., 2022), it is important to highlight that exotic detrital zircon may be derived from IRD that are completely unrelated to the presence of continental fragments at depth. The combined influences of the EGC and EIC, modulated by the colder climatic conditions of the LALIA, likely facilitated Greenlandic IRD deposition along Iceland's coastal margins. Isostatic uplift following rapid deglaciation in the Breiðafjörður region further influenced the placement of these materials, resulting in raised terraces (Brader et al., 2017) that record the far-reaching effects of glacial and oceanic interactions in the North Atlantic during the LALIA.

ACKNOWLEDGEMENTS

This manuscript benefited from discussions with Tamara Carley and financial support from Zheng-Xiang Li. We also appreciate the analytical support received from Noreen Evans and Brad McDonald of the John de Laeter Centre at Curtin University. Comments from Dr. James S Eldrett and an anonymous reviewer greatly improved the manuscript.

FIGURES

Figure 1. Raised beach with exotic clasts at Breiðavík, northwest Iceland. (A) Satellite image of Iceland with insets of the Breiðavík region. The dashed line corresponds to the location of the lower terrace where the samples were collected (65.547945° N, -24.381130° W). (B) Drone oblique view looking south across the beach terraces. Footprints, tire tracks, and person for scale in foreground, center, and background, respectively. (C) Example of an exotic clast found within the lower terrace.

Figure 2. Location of potential source regions of Greenland-derived IRD of the Breiðavík clasts found in Iceland shown on a simplified geologic map of Greenland (White et al., 2016). Dashed lines denote Greenland bedrock provinces. Solid lines denote Greenland ice sheet watersheds. Black arrows denote ocean currents. EGC—East Greenland current. EIC—East Icelandic current. IC—Irminger current.

Figure 3. Fingerprinting the Greenlandic provenance of the exotic Breiðavík clasts. εHf versus age plot of zircon from the Breiðavík clasts. Compiled Greenlandic detrital zircon were extracted from the database of Puetz et al., (2024) with data from Johnston and Kylander-Clark, (2013); Nicoli et al., (2018); Olierook et al., (2020).

REFERENCES

Batchelor, C.L., Margold, M., Krapp, M., Murton, D.K., Dalton, A.S., Gibbard, P.L., Stokes, C.R., Murton, J.B., and Manica, A., 2019, The configuration of Northern Hemisphere ice sheets through the Quaternary: Nature Communications, v. 10, p. 3713, doi:10.1038/s41467-019-11601-2.

Black, L.P., Kamo, S.L., Allen, C.M., Davis, D.W., Aleinikoff, J.N., Valley, J.W., Mundil, R., Campbell, I.H., Korsch, R.J., and Williams, I.S., 2004, Improved 206Pb/238U microprobe geochronology by the monitoring of a trace-element-related matrix effect; SHRIMP, ID–TIMS, ELA–ICP–MS and oxygen isotope documentation for a series of zircon standards: Chemical Geology, v. 205, p. 115–140.

Bond, G., Broecker, W., Johnsen, S., McManus, J., Labeyrie, L., Jouzel, J., and Bonani, G., 1993, Correlations between climate records from North Atlantic sediments and Greenland ice: Nature, v. 365, p. 143–147.

Bond, G., Kromer, B., Beer, J., Muscheler, R., Evans, M.N., Showers, W., Hoffmann, S., Lotti-Bond, R., Hajdas, I., and Bonani, G., 2001, Persistent solar influence on North Atlantic climate during the Holocene: Science, v. 294, p. 2130–2136.

Brader, M.D., Lloyd, J.M., Barlow, N.L., Norðdahl, H., Bentley, M.J., and Newton, A.J., 2017, Postglacial relative sea-level changes in northwest Iceland: Evidence from isolation basins, coastal lowlands and raised shorelines: Quaternary Science Reviews, v. 169, p. 114–130.

Brueckner, H.K., Medaris, L.G., Belousova, E.A., Johnston, S.M., Griffin, W.L., Hartz, E.H., Hemming, S., Ghent, E., and Bubbico, R., 2016, An Orphaned Baltic Terrane in the Greenland Caledonides: A Sm-Nd and Detrital Zircon Study of a High-Pressure/Ultrahigh-Pressure Complex in Liverpool Land: The Journal of Geology, v. 124, p. 541–567, doi:10.1086/687552.

Büntgen, U., Crivellaro, A., Arseneault, D., Baillie, M., Barclay, D., Bernabei, M., Bontadi, J., Boswijk, G., Brown, D., and Christie, D.A., 2022, Global wood anatomical perspective on the onset of the Late Antique Little Ice Age (LALIA) in the mid-6th century CE: Science Bulletin, v. 67, p. 2336–2344.

Büntgen, U., Myglan, V.S., Ljungqvist, F.C., McCormick, M., Di Cosmo, N., Sigl, M., Jungclaus, J., Wagner, S., Krusic, P.J., and Esper, J., 2016, Cooling and societal change during the Late Antique Little Ice Age from 536 to around 660 AD: Nature geoscience, v. 9, p. 231–236.

Eldrett, J.S., Harding, I.C., Wilson, P.A., Butler, E., and Roberts, A.P., 2007, Continental ice in Greenland during the Eocene and Oligocene: Nature, v. 446, p. 176–179, doi:10.1038/nature05591.

Foulger, G.R., Gernigon, L., and Geoffroy, L., 2022, Icelandia, in In the Footsteps of Warren B. Hamilton: New Ideas, Geological Society of America Special Papers 434.

Gilbert, R., 1990, Rafting in glacimarine environments: Geological Society, London, Special Publications, v. 53, p. 105–120.

Jackson, S.E., Pearson, N.J., Griffin, W.L., and Belousova, E.A., 2004, The application of laser ablation-inductively coupled plasma-mass spectrometry to in situ U–Pb zircon geochronology: Chemical Geology, v. 211, p. 47–69, doi:10.1016/j.chemgeo.2004.06.017.

Johnston, S.M., and Kylander-Clark, A.R.C., 2013, Discovery of an Eo-Meso-Neoarchean terrane in the East Greenland Caledonides: Precambrian Research, v. 235, p. 295–302, doi:10.1016/j.precamres.2013.07.004.

Kjær, K.H. et al., 2022, Glacier response to the Little Ice Age during the Neoglacial cooling in Greenland: Earth-Science Reviews, v. 227, p. 103984, doi:10.1016/j.earscirev.2022.103984.

Nicoli, G., Thomassot, E., Schannor, M., Vezinet, A., and Jovovic, I., 2018, Constraining a Precambrian Wilson Cycle lifespan: An example from the ca. 1.8Ga Nagssugtoqidian Orogen, Southeastern Greenland: Lithos, v. 296–299, p. 1–16, doi:10.1016/j.lithos.2017.10.017.

Olierook, H.K.H., Barham, M., Kirkland, C.L., Hollis, J., and Vass, A., 2020, Zircon fingerprint of the Neoproterozoic North Atlantic: Perspectives from East Greenland: Precambrian Research, v. 342, p. 105653, doi:10.1016/j.precamres.2020.105653.

Paton, C., Hellstrom, J., Paul, B., Woodhead, J., and Hergt, J., 2011, Iolite: Freeware for the visualisation and processing of mass spectrometric data: Journal of Analytical Atomic Spectrometry, v. 26, p. 2508–2518.

Puetz, S.J., Spencer, C.J., Condie, K.C., and Roberts, N.M., 2024, Enhanced U-Pb detrital zircon, Lu-Hf zircon, δ18O zircon, and Sm-Nd whole rock global databases: Scientific Data, v. 11, p. 56.

Rehnström, E.F., 2010, Prolonged Paleozoic Magmatism in the East Greenland Caledonides: Some Constraints from U-Pb Ages and Hf Isotopes: The Journal of Geology, v. 118, p. 447–465, doi:10.1086/655010.

Røhr, T.S., Andersen, T., Dypvik, H., and Embry, A.F., 2010, Detrital zircon characteristics of the Lower Cretaceous Isachsen Formation, Sverdrup Basin: Source constraints from age and Hf isotope data: Canadian Journal of Earth Sciences, v. 47, p. 255–271.

306 Savkina, K., Bashirova, L., and Novichkova, E., 2018, Changes in surface conditions
307 east of the Reykjanes Ridge (North Atlantic) during the Late Pleistocene to Holocene
308 cold events: Russian Journal of Earth Sciences, v. 18, p. 1–12.
309 Spencer, C., Kirkland, C., Roberts, N., Evans, N., and Liebmann, J., 2020, Strategies
310 towards robust interpretations of in situ zircon Lu–Hf isotope analyses: Geoscience
311 Frontiers, v. 11, p. 843–853.
312 White, L.F., Bailey, I., Foster, G.L., Allen, G., Kelley, S.P., Andrews, J.T., Hogan, K.,
313 Dowdeswell, J.A., and Storey, C.D., 2016, Tracking the provenance of Greenland-
314 sourced, Holocene aged, individual sand-sized ice-rafted debris using the Pb-isotope
315 compositions of feldspars and 40Ar/39Ar ages of hornblendes: Earth and Planetary
316 Science Letters, v. 433, p. 192–203, doi:10.1016/j.epsl.2015.10.054.
317 Wiedenbeck, M., Hanchar, J.M., Peck, W.H., Sylvester, P., Valley, J., Whitehouse, M.,
318 Kronz, A., Morishita, Y., Nasdala, L., and Fiebig, J., 2004, Further characterisation of the
319 91500 zircon crystal: Geostandards and Geoanalytical Research, v. 28, p. 9–39.

Figures

Figure 1.

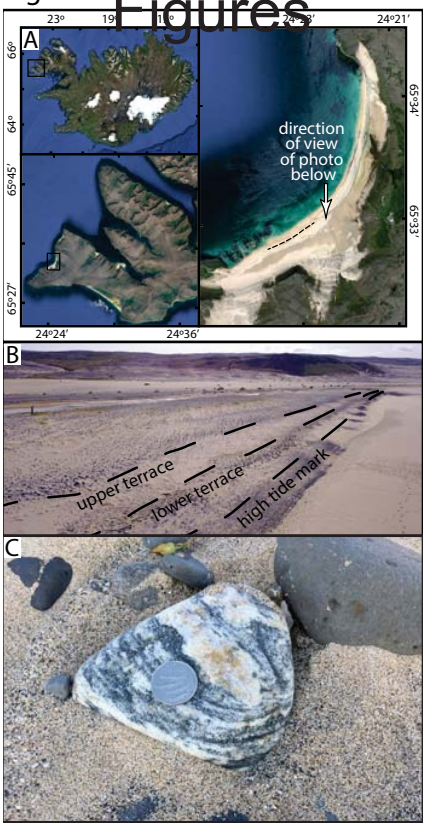

Figure 2.

Figures

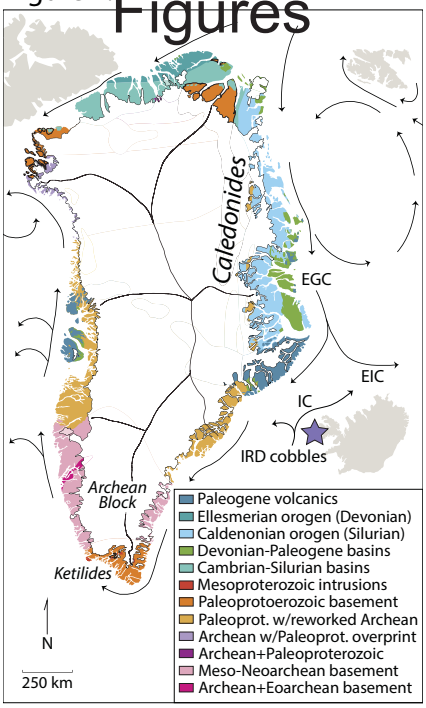

Figures

Figure 3.